International Journal of Science Academic Research
Vol. 06, Issue 03, pp.9653-9661, March, 2025
Available online at http://www.scienceijsar.com

ISSN: 2582-6425

Research Article

ADSORPTION OF A BASIC ORGANIC DYE METHYLENE BLUE IN AQUEOUS SOLUTION ON A LOW-COST BIOSORBENT BASED ON *PERSEA AMERICANA* MILL KERNELS

Emmanuel ORIA MATESO, Bernick WEMBOLOWA TSHENE, Kifline MILEBUDI KIFUANI, *Anatole KIA MAYEKO KIFUANI, Leon-Brejnev MUNYARUKA BALAGA, Pitchou BOKOLOMBE NGOY and Gracien BAKAMBO EKOKO

Laboratory of Physical Organic Chemistry, Water and Environment, Department of Chemistry and Industry, Faculty of Sciences and Technology, University of Kinshasa, P.O. Box 190 Kinshasa XI, Democratic Republic of Congo

Received 20th January 2025; **Accepted** 25th February 2025; **Published online** 31st March 2025

Abstract

The removal of methylene blue (MB) in aqueous solution was studied by adsorption on a biosorbent made from *Persea americana* Mill kernels (PAB) to evaluate its capacity to the adsorption of organic dyes, water pollutants. The adsorption was studied in batch mode by varying several adsorption parameters including dose of adsorbent, contact time, initial concentration and pH of MB solution. After stirring and centrifuging the supernatant was analyzed with a UV-Vis spectrophotometer. The results obtained in this research showed that the biosorbent PAB has a pH_{ZPC} of 4.27, a specific surface area of 102.86 $m^2\ g^{-1}$ and a maximum observed adsorption capacity (Q_{mo}) of 31.22 mg g^{-1}. The adsorption capacity and the percentage of adsorption for different masses of biosorbent, initial concentration and pH of methylene blue solution increase with the time of contact. This increase is due to the availability of free sites of adsorption on the surface of the biosorbent. The maximum adsorption capacity (Q_m) of the biosorbent shows a decrease when the mass of the biosorbent increases; on the other hand, the maximum adsorption capacity ($\%_m Ads$) shows an increase when the mass of the biosorbent increases. This decrease is due to the mass effect of the biosorbent and the increase is due to availability of free sites with an increase in the mass of the biosorbent. The optimal adsorption weight was evaluated at 600 mg and an optimum pH of 10.16, with a maximum adsorption percentage of 98.67%, after 120 minutes. The kinetic and equilibrium results obtained in this study show that the pseudo-first-order model ($R_g^2 = 0.9164$) is better compared to the pseudo-second-order model ($R_g^2 = 0.9045$) to describe the adsorption kinetic of MB on the PAB biosorbent, and, the Freundlich equilibrium model ($R_g^2 = 0.9619$) is better to describe the adsorption equilibrium of MB on the biosorbent PAB compared to Langmuir model ($R_g^2 = 0.9527$). The Langmuir separation parameter $R_L$and the Freundlich 1/*n* parameter, less than 1, suggest that the adsorption of MB on PAB biosorbent is favorable. The biosorbent PAB offers a high potential for adsorption of dyes in aqueous solutions.

Keywords: *Persea Americana* Mill kernels, Methylene Blue, Adsorption, Biosorbent, Isotherm, Kinetic.

INTRODUCTION

Organic dyes are widely used by several industries including textile, wood, paper and plastic industries. Nearly 15 to 20% of the dyes used for dyeing textiles are discharged through water effluent without prior treatment (Alouani *et al.,* 2018). Mekhalef *et al*. (2018) reported that the discharge of water loaded with organic dyes from industries presents significant risks for human health and the aquatic ecosystem. Organic dyes induce environmental pollution and give water pestilential odors and noticeable discolorations. They induce intoxication of aquatic species and humans through the trophic chain (Vanessa *et al.,* 2017; Kifuani *et al.,* 2018a ;Merbouh, *et al.* , 2020 ; Li *et al.,* 2021;Jan *et al.,* 2022). Methylene blue (MB), a cationic thiazine dye, is one of the organic dyes widely used in textile industry. It is used for dyeing cotton, wood and silk. It is also used as chemical indicator, biological stain, and drug (Pathirana *et al.,* 2017; Jia *et al.,* 2018; Nworie *et al.,* 2019). By contact, inhalation or ingestion, methylene blue can induce breathing difficulties, burning sensations in the mouth, nausea, vomiting, diarrhea, gastroenteritis, perspiration, cold sweats, permanent injury to the eyes of humans and animals.

Corresponding Author:** ***Anatole KIA MAYEKO KIFUANI,
Laboratory of Physical Organic Chemistry, Water and Environment, Department of Chemistry and Industry, Faculty of Sciences and Technology, University of Kinshasa, P.O. Box 190 Kinshasa XI, Democratic Republic of Congo

The removal of methylene blue and other dyes from effluents is important for environmental and human health (Rahimian and Zarinabadi, 2020; Nyakairu *et al.,* 2024). Several methods have been developed for dyes removal classified into biological, chemical and physical methods, including a variety of techniques such as: adsorption, advanced oxidation, biosorption, chemical and electrochemical oxidation, coagulation, filtration, flocculation, microbial and fungal decolorization, photocatalysis, nanofiltration, ozonation, reverse osmosis (Kifuani *et al.,* 2018b ; Mekky *et al.,* 2020 ; Basma *et al.,* 2023 ; Raiyyaan *et al.,* 2024). Ali *et al.* (2021), Tshene *et al.*(2024) reported that many of these techniques have proven to be expensive or responsible for the pollution induced because of the degradation products formed, sometimes more toxic than the initial dyes themselves. Rahimian and Zarinabadi (2020) showed that among the processes for treating water polluted by organic dyes, adsorption turns out to be the most effective. Activated carbon is generally the most widely used adsorbent. But in some cases, it requires regeneration, a complex and expensive operation (Razia *et al.,* 2022). Nowadays, different agricultural wastes are tested as low-cost adsorbents for the removal of organic dyes from water. These include the biomass of rattan sawdust, cotton stalk, hazelnut shell, oil palm shell, coffee residue, orange peel, powdered peanut hull, sugarcane bagasse, sunflower stalks, mango seed kernel, coconut coir dust, apricot stones, groundnut shells, banana pith, yellow passion fruit

waste, green pea peels, mango leaves, *Hevea brasilliensis* seed coat, coir pith and Peach stones. These materials contain organic substances such as polyphenols, lignin, tannins, pigments and protein which provide surface functions, such as carboxylic acid, ketone, aldehyde, phenol, lactone, pyrone, responsible for the adsorption of organic compounds or other pollutants on their surface (Pathiana *et al.,* 2017 ; Jia *et al,* 2018 ; Ahmad *et al.,* 2019 ; Mobalayi *et al.,* 2021; Hatiya *et al.,* 2022 ; Basma *et al.,* 2023 ; Gani *et al.,* 2023 ; Tshene *et al.,* 2024). In this study, *Persea americana* Mill kernels powder, a low-cost material, was used as bioadsorbent to evaluate its ability to removal methylene blue in an aqueous solution. The effects of different adsorption parameters were studied including dose of adsorbent, contact time, initial concentration and pH of methylene blue solution.

MATERIALS AND METHODS

Adsorbate and adsorbate solutions

Methylene blue, a cationic thiazine dye, is widely used for the characterization of adsorbent. It has a flat surface of 175 $Å^2$. His IUPAC name is 3,7- Bis (dimethylamino) phenothiazin- 5-ium chloride. Its chemical formula is $C_{16}H_{18}N_3SCl$ and Mw 319.852 g mol^{-1}. Methylene blue used in this study was obtained from Merck and used without purification. All the reagents used in this study were of analytical grade. Figure 1 shows the structure of methylene blue.

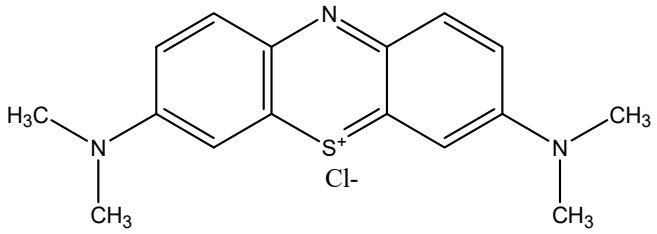

Figure 1. Structure of Methylene Bleu

Methylene blue solutions were prepared by dissolving MB crystals in distilled water and diluting the resulting solution to obtain solutions ranging from 1 mg L^{-1} to 100 mg L^{-1}. The pH of the MB solutions was adjusted by adding 0.1 N HCl or 0.1 N NaOH solutions to obtain solutions ranging from pH 2 to 12. The MB solutions, before and after adsorption, were analyzed using a UV-Vis spectrophotometer (HACK Spectrophotometer, SP, model 1105) at maximum length wave, determined experimentally, by scanning in the range of 400 nm to 700 nm, for each pH studied in this paper. The residual concentration was calculated from the Beer-Lambert law, giving by equation 1(Raiyyaan *et al.,* 2021):

$$A = \varepsilon.l.C \quad (1)$$

With, A being the absorbance, ε the molar absorption coefficient (L mg^{-1} cm^{-1}), l the thickness of the cell (1 cm) and C, the concentration of the solute (mg L^{-1}).

Preparation and characterization of the biosorbent (PAB)

The biosorbent was prepared from *Persea americana* Mill kernels collected from the city of Mbanza Ngungu, Province of Kongo Central, Democratic Republic of Congo. The kernels were first washed with distilled water, dried in an oven at 105°C (DESPATCH Oven Co, type Elect). crushed and then sieved to obtain a fine powder (≤500 µm). The *Persea americana* biosorbent (PAB) thus obtained were stored in a desiccator at laboratory temperature (28°C), to keep it free from moisture contact and oxidation (Kifuani *et al.,* 2018a). The bioadsorbent was characterized by the determination of Humidity, Dry matter, Ash and pH_{ZPC}.

Humidity and dry matter

Humidity (H) and dry matter (DM) were determined by loss of weight after heating 5 g of PAB in a oven. The humidity level (%H) was calculated by the following relationship (Ajala *et al.,* 2024):

$$\%H = \frac{(m_1 - m_2) \cdot 100}{m_1} \quad [2]$$

Where, m_1 and m_2, the weights of biosorbent before and after steaming, respectively.

The dry matter level (%DM) was determined after deducting the humidity level from 100% of the initial sample.

Ash content

The ash content was evaluated by determining the weight loss after calcination of 5 g of PAB in a muffle furnace (NABER, Model N7/H) for 8 hours. The ash content (%A) was calculated according to equation 3 (Basma *et al.,* 2023):

$$\%A = \frac{(m_3 - m_4) \cdot 100}{m_3} \quad [3]$$

Where, m_3 and m_4, the weights of biosorbent before and after calcination, respectively.

Determination of pH_{ZPC}

The pH drift method was used for the determination of the zero point of charge (pH_{ZPC}) (Kifuani *et al.,* 2012; Musah *et al.,* 2020). For this purpose, 100 mL of 0.01 mol L^{-1} NaCl solution were placed in different Adsorbers (LACOPE ADX). The pH of these solutions was adjusted from 2 to 12, by addition of 0.1 N HCl or 0.1 N NaOH solutions, to adjust the acidic or basic solutions, respectively. 1000 mg of biosorbent are then added to each solution and the suspension was stirred for 72 h and centrifuged at 3000 rpm (Centrifuge Labofuge 200 Heraeus). A pH-Meter (Hanna Instrument) was used to determine the final pH of the solutions after centrifugation. The pH_{ZPC} is given by the intersection of the curve obtained by plotting the final pH as a function of the initial pH of each solution.

Determination of specific surface area

The specific surface area (S_{BM}) was evaluated by the Kifuani method, Kifuani volume variation method (KVVM), which consists of studying, at equilibrium time, the adsorption of methylene blue with a low weight of biosorbent (5 mg) using increasing volumes (100 mL to 1000 mL) of MB solutions (50 mg L^{-1}). The plateau obtained by plotting the adsorption capacity (q_e) as a function of the volume (V) of the MB solution corresponds to the maximum observed adsorption capacity (q_{mo} or Q_{mo}) (Kifuani *et al.,* 2012; Kifuani, 2013; Kifuani *et al.,* 2018a). The specific surface area (S_{MB}) was then

calculated using the following equation 4 (Kifuani *et al.,* 2012):

$$S_{MB} = Q_{mo} \cdot N_A \cdot s \quad [4]$$

Where, S_{MB} being the specific surface area determined using MB as adsorbate (m^2 g^{-1}), Q_{mo} the maximum observed adsorption capacity (mg g^{-1}), N_A the Avogadro number (6.022 10^{23} mol^{-1}) and *s*, the area occupied by a MB molecule (175 $Å^2$).

Batch adsorption experiments

The adsorption tests were carried out with different concentrations (5 mg L^{-1} -100 mg L^{-1}) and pH (2 – 12) of methylene blue solutions and different masses (1 mg – 1000 mg) of bio adsorbents. Adsorption was also been studied at different contact times (0 - 390 minutes). The pH of the MB solutions was adjusted by adding a solution of 0.1N of HCl or 0.1N of NaOH, to adjust the acidic or basic solutions respectively.

Before use, the PAB biosorbent was dried in an oven at 105°C for 3 h and the mass of the biosorbent was determined by weighting using an analytical balance (HEB-E 303). The adsorption tests were carried out in an adsorber (LACOPE ADS) with 100 mL of MB solution. After stirring for the required time, the suspension was centrifuged at 3000 rpm for 30 minutes and the supernatant was analyzed with a UV-Vis spectrophotometer at the appropriate wavelength, to determine the residual concentration of the MB solution. Each experiment is repeated three times to determine the absolute error. Equations 5 and 6 were used to calculate the adsorption capacity (Q_e) and adsorption percentage (%*Ads*) respectively (Mobalaji *et al.,* 2021):

$$Q_e = \frac{(C_o - C_e)V}{m_B} \quad [5]$$

$$\%\, Ads = \frac{C_o - C_e}{C_o} x\,100 \quad [6]$$

With, Q_e being the apparent adsorption capacity or the equilibrium capacity of the biosorbent (mg g^{-1}), C_o the initial concentration of methylene blue solution (mg L^{-1}), C_e the residual or equilibrium concentration (mg L^{-1}), *V* the volume of the methylene blue solution (L) and %*Ads*, the adsorption percentage.

Adsorption kinetics

The pseudo-first-order and pseudo-second-order kinetic models of Lagergren, giving by equations 7 to 10, were used to describe the adsorption kinetic of MB on the PAB biosorbent (Mekky *et al.,* 2020):

Lagergren Pseudo-first-order model:

$$\frac{dq_t}{dt} = k_1(q_e - q_t) \quad [7]$$

$$\ell n(q_e - q_t) = \ell n\, q_e - k_1 t \quad [8]$$

Lagergren Pseudo-second-order model

$$\frac{dq_t}{dt} = k_2(q_e - q_t)^2 \quad [9]$$

$$\frac{1}{(q_e - q_t)} = \frac{1}{q_e} + k_2 t \quad [10]$$

In this study, pseudo-first-order and pseudo-second-order model equations modified by Kifuani were used, using the following equations 11 and 12 (Kifuani *et al*, 2012; Kifuani, 2013):

Kifuani Pseudo-first- order kinetic model:

$$\ell n \frac{q_e}{(q_e - q_t)} = k_1 t \quad [11]$$

With, q_e being adsorption capacity at equilibrium (mg g^{-1}), q_t adsorption capacity at time *t* (mg g^{-1}), q_e-q_t adsorption capacity of free sites, *t* the time (s) and k_1, the constant rate of pseudo-first order reaction (min^{-1}).

The plot of $\ell n \frac{q_e}{(q_e - q_t)}$ versus *t* gives a line whose slope corresponds to k_1, the rate constant of pseudo-first-order reaction.

Kifuani Pseudo-second-order kinetic model:

$$\frac{q_t}{q_e(q_e - q_t)} = k_2 t \quad [12]$$

Where, k_2 is the rate constant of the pseudo- second- order reaction (g mg^{-1} min^{-1}).

The plot of $\frac{q_t}{q_e(q_e - q_t)}$ versus *t*, give a line whose slope corresponds to k_2, the rate constant of the pseudo-second–order reaction.

Adsorption isotherms

The adsorption isotherms were determined for pH 2 to 12 by application of linear models of Langmuir and Freundlich, giving by the following equations 13 and 15 (Alouani *et al.,* 2018):

Langmuir model:

$$\frac{1}{Q_e} = \frac{1}{Q_m} + \frac{1}{Q_m K_L} \cdot \frac{1}{C_e} \quad [13]$$

Where, Q_e is the apparent adsorption capacity of the biosorbent (mg g^{-1}), Q_m the adsorption capacity at saturation or maximum adsorption capacity (mg g^{-1}), K_L equilibrium constant adsorption (L mg^{-1}) and *C*e, equilibrium concentration.

The plot of $1/Q_e$ versus $1/C_e$ gives a line which allows to determine Q_m and K_L, from the intercept and slope, respectively.

The Langmuir separation parameter (R_L) was calculated by the following equation (Hajir *et al.,* 2024):

$$R_L = \frac{1}{1 + K_L C_o} \quad [14]$$

With, K_L being the Langmuir constant (L mg^{-1}) and C_o the initial dye concentration.

Freundlich model:

$$\text{Log } Q_e = \log K_F + \frac{1}{n} \log C_e \quad [15]$$

Where, Q_e the adsorption capacity at equilibrium (mg g^{-1}), K_F the adsorption constant (Freundlich constant), C_e the concentration of the adsorbate at equilibrium (mg L^{-1}) and n, the Freundlich constant, characterizing the affinity of solute for the adsorbent (affinity parameter).

The plot of log Q_e versus log C_e gives a line which allows to determine K_F and $1/n$ from the intercept and slope, respectively.

RESULTS

Characteristics of the biosorbent PAB

The physicochemical characteristics of PAB biosorbent are given in Table 1. These results indicate that the biosorbent has a specific surface area of 102.86 m^2 g^{-1} and a maximum observed adsorption capacity (Q_{mo}) of 31.22 mg/g. The pH_{ZPC} of the adsorbent is 4.27.

Tableau 1.Characteristics of PAB biosorbent

Parameters	Values
Particule size (µm)	≤ 500
Ash (%)	3.28
Humidity (%)	6.50
Dry matter (%)	93.50
pH_{ZPC}	4.27
Q_{mo} (mg g^{-1})	31.22
Specific area, S_{MB} (m^2 g^{-1})	102.86

Effect of biosorbent dosage

The optimal mass to remove methylene blue was determined by placing in a stirrer 100 mL of MB solution 50 mg L^{-1}, at self-equilibrium pH (6.05) with different masses of biosorbent at the equilibrium time. The results obtained are shown in Table 2 and Figures 2 and 3. The results of Figure 2 show a decrease in the maximum capacity (Q_m) when the mass of the biosorbent increases from 5 to 1000 mg. Figure 3, on the other hand, shows an increase in the maximum percentage of adsorption when the mass of the biosorbent increases. The results reported in Figure 3 show that when the weight of the biosorbent increases, from 5 to 1000 mg, the maximum percentage adsorption ($\%_m Ads$) also increases from 58.33% to 98.00%. The optimal adsorption weight was evaluated to be 600 mg, with a maximum adsorption percentage of 98.00%, after 120 min. After this weight, the adsorption tends towards constancy.

Tableau 2. Equilibrium concentration (C_e), maximum adsorption capacity (Q_m), maximum percentage of adsorption ($\%_m Ads$) and equilibrium time (t_e) at differents wheights of biosorbent (m_{PAB})

m_{PAB}	C_e (mg L^{-1})	Q_m (mg g^{-1})	$\%_m Ads$	t_e (min)
5	20.83	583.33	58.33	270
20	12.30	187.50	75.00	270
50	9.83	80.33	80.83	270
100	3.67	46.33	92.67	270
200	2.00	24.00	96.00	260
400	1.83	12.04	96.33	120
600	1.17	8.00	97.17	120
800	1.17	6.10	97.67	120
1000	1.00	4.89	98.00	120

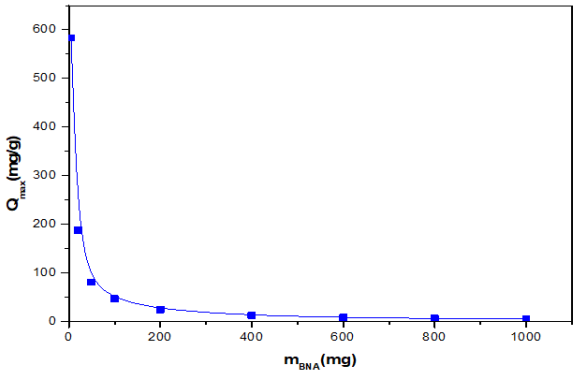

Figure 2. The maximum adsorption capacity (Q_m) vs dose of biosorbent (m_{PAB})

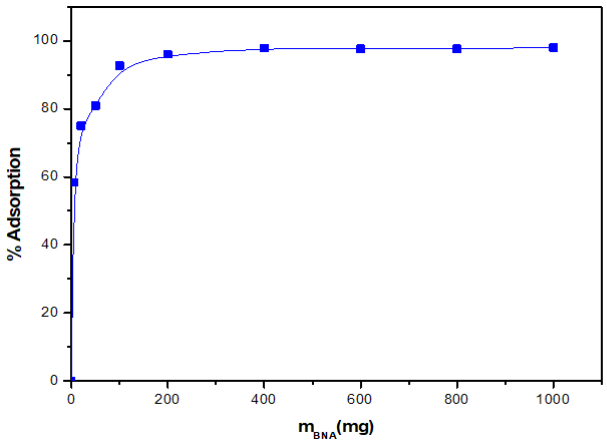

Figure 3. The maximum percentage of adsorption ($\%_m Ads$) vs dose of biosorbent (m_{PAB})

Effect of contact time

The adsorption tests were carried out from 0 to 390 minutes, first with a methylene blue solution 50 mg L^{-1} for different weights of adsorbent, after, with different initial concentrations and pH of BM solutions using 600 g of PAB. The results obtained are given by Table 2, and Figures 4 to 9. The results obtained show that the capacity and percentage of adsorption of MB on PAB increase with contact time. The curves obtained present three phases: the first phase is very rapid at the beginning during the first 10 minutes; then a second with a low speed and finally a third represented by a horizontal line of the adsorption capacity or the percentage of adsorption.

.

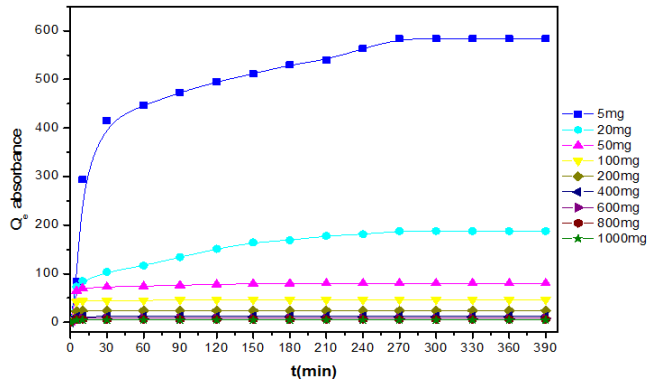

Figure 4. Effect of contact time (*t*) on the adsorption capacity (Q_e) of PAB at different dose of biosorbent

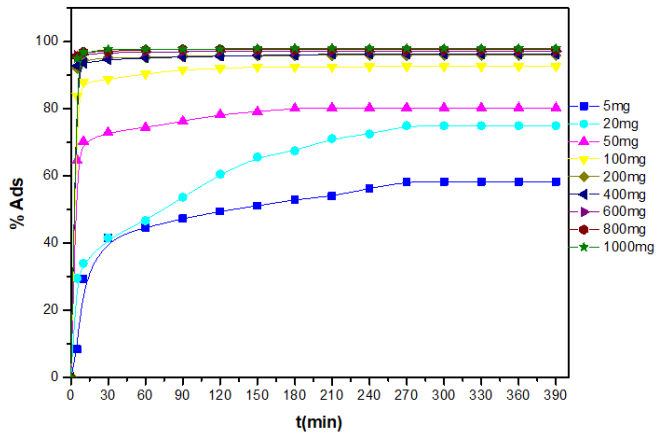

Figure 5. Effect of contact time (*t*) on the percentage (%Ads) of MB adsorption on PAB at different dose of biosorbent

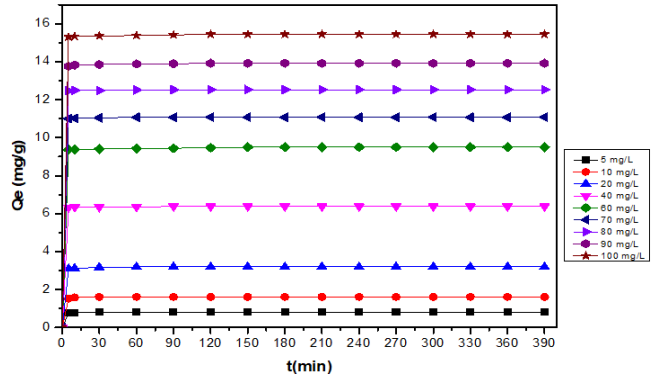

Figure 6. Effect of contact time (*t*) on the adsorption capacity (Q_e) of PAB at different initial concentrations of MB solution

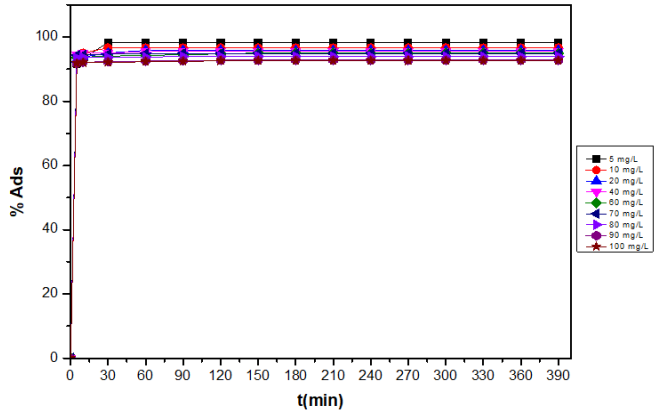

Figure 7. Effect of contact time (*t*) on the percentage of MB adsorption (%Ads) at different initial concentrations of MB solution

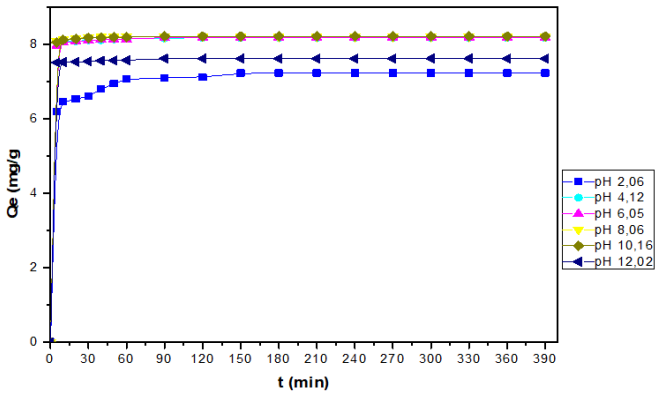

Figure 8. Effect of contact time (*t*) on the adsorption capacity (Q_e) of PAB at different pH of MB solution

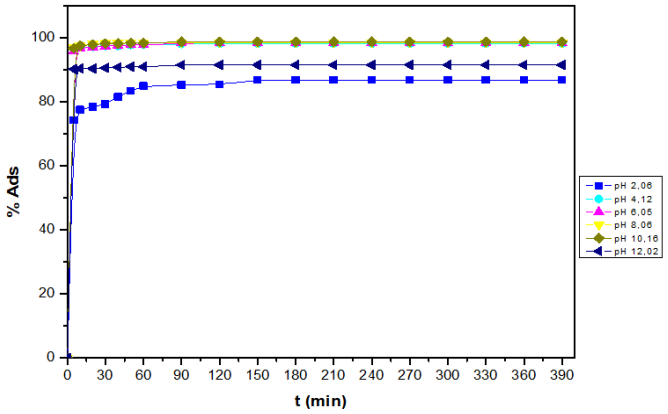

Figure 9. Effect of contact time (*t*) on the percentage of MB adsorption (%*Ads*) on PAB at different pH of MB solution

Effect of initial Methylene blue concentration

Figures 10 and 11 show the effect of the initial concentration of the methylene blue solution on the maximum adsorption capacity and the maximum adsorption percentage of the bioadsorbent PAB. The results presented in Figures 10 and 11 show that the maximum adsorption capacity of the PAB biosorbent increases with the initial concentration of the BM solution without reaching the saturation level in the range of concentrations studied (Figure 10), the maximum adsorption percentage of the biosorbent decreases when the initial concentration of BM increases (Figure 11).

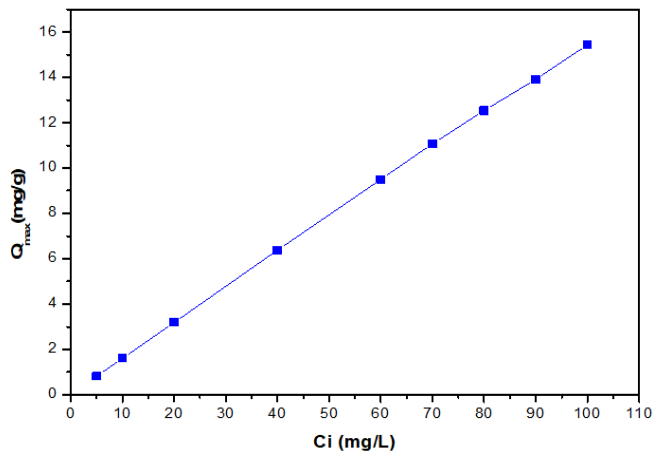

Figure 10. Effect of initial concentration (C_O) on the maximum adsorption capacity (Q_m) of PAB

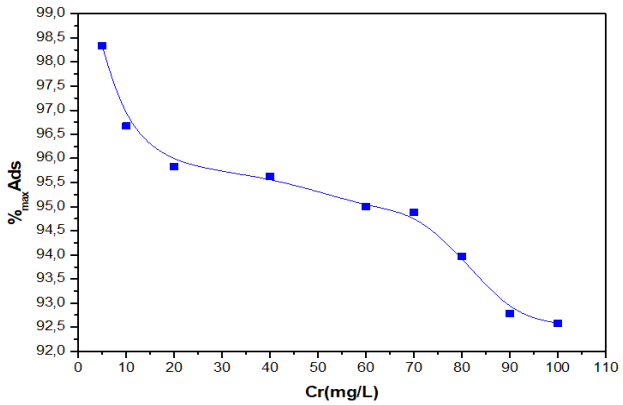

Figure 11. Effect of initial concentration (C_O) on the maximum adsorption percentage ($\%_m Ads$) of PAB

Effect of pH

The effect of MB pH solution on the adsorption is given by Table 3, Figures 12 and 13. These results reported that the maximum adsorption capacity and the maximum adsorption percentage increase with the pH of MB solution and tend to a constant value after pH 6.05, with a maximum adsorption capacity of 8.22 mg/g and a maximum adsorption percentage of 98.67%, after 90 minutes at pH 10.16.

Tableau 3. Maximum adsorption capacity (Q_m), maximum percentage of adsorption ($\%_m Ads$), and equilibrium time (t_e) at different pH

pH	Q_m (mg/g)	$\%_m Ads$	t (min)
2.06	7.23	86.77	150
4.12	8.18	98.15	120
6.05	8.19	98.29	90
8.06	8.21	98.53	90
10.16	8.22	98.67	90
12.06	7.62	91.45	150

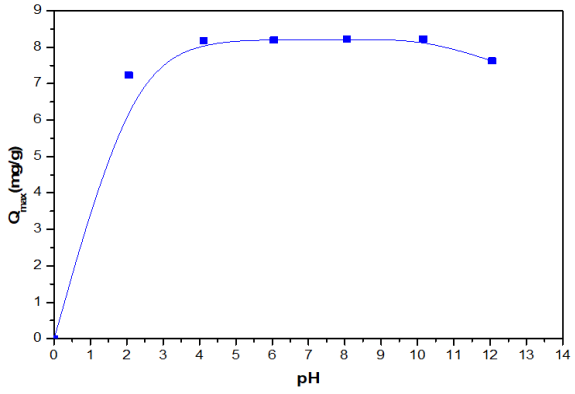

Figure 12. Effect of pH of MB solution on maximum adsorption capacity (Q_m) of PAB

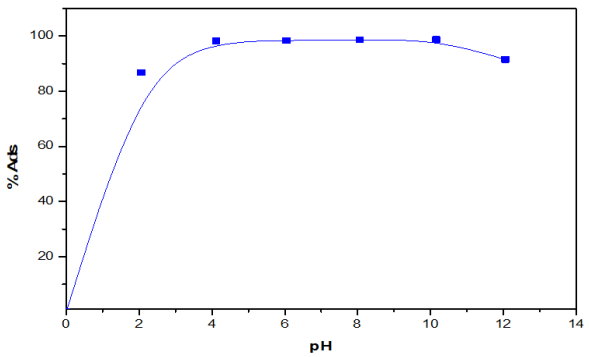

Figure 13. Effect of pH of MB solution on the maximum adsorption percentage ($\%_m$Ads) of PAB

Modeling of adsorption kinetics

The results of the modeling of the adsorption kinetics of methylene blue on PAB biosorbent, according to the kinetic models of pseudo-first-order and pseudo-second-order, are given in Table 4. From these results we can observe that, at different pH, the k_1 constants range from 0.0169 min^{-1} to 0.1105 min^{-1}, while the k_2 values range from 0.0792 g mg^{-1} min^{-1} to 4.2620 g mg^{-1} min^{-1}.

Tableau 4. Pseudo-first-order and pseudo-second-order parameters for adsorption of MB onto PAB at different pH

pH	Pseudo-first-order parameters		Pseudo-second-order parameters	
	k_1 (min^{-1})	R^2	k_2 (g mg^{-1} min^{-1})	R^2
2.06	0.0198	0.8707	0.0792	0.9114
4.16	0.0276	0.9599	0.9504	0.7499
6.05	0.0254	0.9053	0.2927	0.9626
8.06	0.1105	0.9553	4.2620	0.8834
10.16	0.0287	0.8483	0.5114	0.9362
12.06	0.0169	.0.9586	0.2804	0.9837
R_g^2		0.9164		0.9045

R_g^2 :overall linear correlation coefficient

Modeling of adsorption isotherms

The adsorption isotherms of BM on the PAB biosorbent at different pH from 2 to 12 were modeled according to the Langmuir and Freundlich equilibrium models. The modeling of the isotherms allowed to determine the parameters of Langmuir (Q_m, K_L, R_L) and Freundlich (K_F , $1/n$) presented in Table 5.

Tableau 5. Langmuir and Freundlich parameters for the adsorption of MBonto PAB at different pH

pH	Q_m (mg/L)	Langmuir parameters			Freundlich parameters		
		K_L (L mg-1)	R_L	R^2	K_f (mg g^{-1}) (mg $L^{-1})^{-1/n}$	$1/n$	R^2
2.06	7.23	1.7827	0.0111	0.9771	3.1036	0.4830	0.9885
4.16	8.18	2.7975	0.0071	0.9480	7.9010	1.1386	0.9105
6.05	8.19	1.9538	0.0101	0.9694	10.3453	0.6813	0.9352
8.06	8.21	1.9301	0.0102	0.9565	10.6272	0.6717	0.9767
10.16	8.22	2.3591	0.0084	0.8804	7.2891	1.4064	0.9573
12.02	7.62	13.2814	0.0015	0.9849	1.0799	0.0463	0.9964
R^2 global				0.9527			0.9619

R_g^2 :overall linear correlation coefficient

DISCUSSION

The maximum observed adsorption capacity (Q_{mo}) of PAB with a value of 31.22 mg g^{-1} (Table 1) is lower compared to that reported by Rahimian and Zarinabadi (2020) with 40.0 mg g^{-1} for the leaves of pine trees biosorbent. The pH_{ZPC} of 4.27 indicates that the surface of the biosorbent is neutral at this pH, positive at a pH lower than 4.27 and negative at pH higher than 4.27. The decrease of the maximum adsorption capacity (Q_m) when the mass of the bioadsorbent increases is due to the mass effect of the biosorbent, making a certain fraction of the biosorbent unavailable for adsorption but taken into account in the calculation of Q_m. On the other hand, the maximum adsorption capacity increases when the mass of the biosorbent increases. This increase is due to availability of free sites with an increase in the mass of the biosorbent. Similar observation was reported by Kifuanit *et al.* (2018a) in studying the adsorption of methylene blue in aqueous solution on a biosorbent from agricultural waste of *Cucumeropsis mannii* Naudin. The increase of the adsorption capacity or the percentage of adsorption of PAB biosorbent with contact time

for different masses of biosorbent, initial concentration and pH of methylene blue solution (Figures 4 to 9) is due to the availability of free sites of adsorption with the increase of these parameters (Ajala *et al.,* 2024). The increase in adsorption capacity and percentage of adsorption is rapid in the first phase. This rapid increase is due to the availability of a large number of free sites in the beginning witch gradually become saturated to reach the maximum apparent adsorption capacity indicated by a horizontal line. At this moment the sites are saturated and the adsorption becomes constant. Other researchers have also reported the same observation (Bouazza, 2012; Nigist *et al.,* 2022; Gani *et al.,* 2023; Kifuani *et al.,* 2024). From the results of Figure 10, it appears that the adsorption capacity of the PAB biosorbent is higher with the increase in the initial dye concentration, this is due to the increase of the phenomenon of diffusion of solute particles with the increase of the initial concentration. The decrease of the maximum percentage adsorption when the MB concentration increase (Figure 11) is due to the agglomeration of the solute particles with the increase of initial concentration (Kifuani *et al.,* 2012; Razia *et al*, 2022). Musah *et al*. (2020) also reported the same observations on the decrease in the adsorption percentage with the concentration of the solution for the adsorption of methylene blue on a biosorbent from *Platanus orientalis* leaf powder. These results are also in agreement with those obtained by Abdallah *et al*. (2016), Benyaba and Alioua (2020) and Razia *et al*. (2022).

The increase in the maximum adsorption capacity and the maximum adsorption percentage with the pH of MB solution is explained by the surface charge of the biosorbent. Below the pH_{ZPC} (= 4.27), the surface of the biosorbent is positive, which leads to repulsive interactions between the surface of the biosorbent and the organic cations of methylene blue, hence the reduction in the capacity and percentage of adsorption observed. Beyond the pH_{ZPC}, the surface of the biosorbent is negatively charged, there are then attractive interactions between the surface of the biosorbent and the organic cations which leads to an increase in the capacity and the percentage of adsorption. pH 10.16 with an adsorption percentage of 98.67% was chosen as the optimum pH for better retention of MB on PAB biosorbent (Table 3, Figures 12 and 13). Our results are in agreement with the work of other researchers for the adsorption of this dye on other adsorbents (Bagheri *et al.,* 2016; Mustapha *et al.,* 019; Adeyi *et al.,* 2020; Alhawtali *et al.,* 2024).

The kinetic results obtained in this study (Table 4), show that the pseudo-first-order model (R_g^2 = 0.9164) is better compared to the pseudo-second-order model (R_g^2 = 0.9045) to describe the adsorption of BM on the PAB biosorbent. Adsorption is therefore mainly governed by the surface reaction, characterized by the attachment of methylene blue molecules to the surface of PAB bioadsorbent (Kifuani, 2013). This correlation, less than 1, does not exclude other adsorption mechanisms. Similar kinetic results have been reported in the literature (Musah *et al.,* 2020). The modelling of the adsorption equilibrium according to the Langmuir and Freundlich equilibrium models (Table 5) shows that Freundlich model (R_g^2 = 0.9619) is better to describe the adsorption of BM on the biosorbent PAB compared to Langmuir model (R_g^2 =.9527). The correlation with Freundlich model suggests multilayer adsorption, which appears at high concentrations of MB solution (Kifuani, 2013). This assumes a heterogeneity of the adsorption surface with sites of different adsorption energies (Boumchita *et al*. 2016; Narayana and Ravi 2019; Tahina *et al.* 2022). Similar results have been reported in the literature (Basma *et al.,* 2023; Gani *et al.,* 2023). Bharath and Senthil (2022) reported the similar result on the adsorption of Red of Alizarin S on activated carbon from avocado kernels. The K_L, equilibrium parameter or separation parameter, indicates the affinity of the biosorbent towards methylene blue, which can be favorable ($0 < R_L < 1$), irreversible ($R_L = 0$), linear ($R_L = 1$) or unfavorable ($R_L > 1$) (Amal *et al.,* 2024). The R_L values obtained < 1, for all pH studied, indicate that the adsorption of MB on PAB biosorbent is favorable (Table 5). The K_F values represent the adsorbent power of the biosorbent, when the concentration (C_e) of BM is unitary. The Freundlich parameter $1/n$ indicate the adsorption intensity or adsorption interaction strength. It is reported that the adsorption can be favorable ($1/n<1$), linear ($1/n = 1$), physical and unfavorable ($1/n>1$) (Basma *et al.,* 2024;Hajir *et al*.,2024). The majority of values of $1/n$ lower than 1 suggest that the adsorption of BM on the PAB bioadsorbent is favorable.

Conclusion

The main objective of this study was to evaluate the adsorption capacity of the biosorbent of *Persea americana* kernels using methylene blue as adsorbate. The adsorption was studied in batch mode by varying several adsorption parameters. The results obtained in this research showed that the biosorbent PAB has a specific surface area of 102.86 $m^2\ g^{-1}$ and a maximum observed adsorption capacity (Q_{mo}) of 31.22 mg g^{-1}. The optimal adsorption weight was evaluated at 600 mg and an optimum pH of 10.16, with a maximum adsorption percentage of 98.67%, after 120 minutes. The adsorption of de MB on the biosorbent PAB is better described by the pseudo-first-order model and the Freundlich equilibrium model. The *Persea americana* kernels biosorbent is a biomaterial that has shown interesting adsorption and can be an alternative for the treatment of wastewater polluted by organic dyes.

Competing interests: The authors declare that they have no competing interests.

Authors' contributions: EOM, BWN, KMK and AKMK are the main investigators of this study and have participated in all the stages of the research. LBMB, GBE and PBN have contributed to data processing and discussion of results.

Acknowledgements: The authors of the manuscript gratefully acknowledge Jerry IKELE KURAYUM and Kifline MILEBUDI KIFUANI family for the facilities provided to Professor Anatole KIA MAYEKO KIFUANI during the final editing of this article in Aurora-Denver, Colorado, USA.

REFERENCES

Ajala, E.O., Aliyu, M.O., Ajala, M.A., Mamba, G., Ndana, A.M., Olatunde, T.S. 2024. Adsorption of lead and chromium ions from electroplating wastewater using plantain stalk modified by amorphous alumina developed from waste cans. Scientific reports, 14:6055. DOI: https://doi.org/10.1038/s41598-024-56183-2.

Ali, K., Javaid, U.J., Ali, Z., Zaghum, M.J. 2021. Biomass-derived adsorbents for dye and heavy metal removal from wastewater. *Adsorption Science and Technology,* 2021:1-14. DOI: https://doi.org/10.1155/2021/9357509.

Alouani, M.E.L., Alehyen, S., Achouri, M.E.L., Taibi, M. 2018. Removal of cationic dye methylene blue from aqueous soution by adsorption on fly ash-based geoplymer. *J. Mater. Envir. Sci.,* 9(1):32-46. DOI: https://dx.doi.org/10.26872/jmes.2018.9.1.5.

Basma, G., Alhogbi, G. S., Al, B. 2023. An investigation of a natural biosorbent for removing methylene blue dye from aqueous solution. *Molecules*, 28 (6): 2785. DOI:https://doi.org/10.3390/molecules 28062785.

Bharath, B.G., Senthil, P. 2022. Adsorptive Removal of Alizarin Red S onto sulfuric acid modified avocado Seeds: Kinetics, Equilibrium, and Thermodynamic studies. *Adsorption Science & Technology,* 2022: ID3137870. DOI: https://doi.org/10.1155/2022/3137870.

Gani, P., Puji, L. 2023. Comparison of two biosorbent beads for methylene blue discoloration in water. *J. Ecol. Eng.,* 24(8):137-145. DOI: https://doi.org/10.12911/22998993/166319.

Hajir, N., Abdelrahman, B.F., Omar, A.S. 2024. Isothermal and kinetics investigation of dibenzothiophene removal from model fuel by activated carbon developed from mixed date seed and PET Wastes. *Journal of Ecological Engineering,* 25(3): 38–52. DOI:https://doi.org/10.12911/22998993/177628.

Hatiya, N.A., Reshad, A.S., Negie, Z.W. 2022. Chemical modification of Neem (Azadirachta indica) biomass as bioadsorbent for removal of Pb2+ ion from aqueous wastewater. *Adsorption Science and Technology,* 2022 :1-18. DOI: https://doi.org/10.1155/2022/7813513.

Jan, S.U., Ahmad, Y., Ali, M., Hussain, Z., Melhi, S. 2022. Adsorptive removal of methylene blue from aqueous solution using sawdust. *Medicom Pharmaceutical Sciences,* 2 (1) : 8-16.

Jia, P., Tan, H., Liu, K., Gao, W. 2018. Removal of methylene blue from aqueous solution by bone char. *Appl. Sci.,* 1903: 1-11. DOI : 10.3390/app8101903.

Kifuani, A.K.M, Noki, P.V., Ndelo, J.D.P,, Mukana, W.M., Ekoko, G.B., Ilnga, B.L., Mukinayi, J.M. 2012. Adsorption de la quinine bichlorhydrate sur charbon actif peu couteux à base de la bagasse de canne à sucre imprégnée de l'acide phosphorique. *Int. J. Biol. Chem. Sci.,* 6(3): 1337-1359. DOI: https : //dx.doi.org/10.4314/ijbcs.v6i3.36.

Kifuani, A.K.M. 2013. Adsorption des composés organiques aromatiques en solution aqueuse sur charbon actif à base des déchets agroindustriels. Thèse de doctorat, Université de Kinshasa.

Kifuani, K.M., Kifuani, A.K.M., Ilinga, B.L., Ngoy, P.B., Monama, T.O., Ekoko, G.B., Mbala; B.M., Muswema, J.LL. 2018a. Adsorption d'un colorant basique Bleu de Methylene en solution aqueuse sur un bioadsorbant issu de dechets agricoles de Cucumeropsis mannii Naudin. *Ind . J. Biol. Chem. Sci.,* 12 (1):558-575. DOI: https : //dx.doi.org/10.4314/ijbcs.v12i1.43.

Kifuani, K.M., Kifuani, A.K.M., Ilinga, B/L., Ngoy, P.B., Monama T.O., Ekoko, G.B., Muswema, J.L.. 2018b. Kinetics and thermodynamic studies adsorption of Methylene Bleu in aqueous solution on a bioadsorbent from Cucumeropsis mannii Naudin waste seeds. *Int. J. Biol.Chem. Sci.,* 12 (5): 2412-2423. DOI: https: //dx.doi.org/10.4314/ijbcs.v12i5.38.

Kifuani, A.K.M., Mbenge, L., Kifuani K.M., Tshene, B. W., Tuluenga M., Zola.2024. Removal of basic organic dye methylene blue from aqueous solution by adsorption onto a low-costbiosorbent made from water hyacinth (Eichhornia crassipes). *International Journal of Science Academic Research,* 05(12): 8728-8736. http :// www.scienceijsar.com

Le, P.T., Bui, H.T., Le, T.H., Nguyen, T.H., Pham, L.A., Nguyen, H.N., Nguyen, Q.S., Nguyen, T.P., Bich, N.T., Duong, T.T., Herrmann, M., Ouillon, Le, T.P.Q. 2021. Preparation and characterization of biochar derived from agricultural by-products for dye removal. *Adsorption Science and Technology,* 2021: 1-21. DOI: https://doi.org/10.1155/2021/9161904.

Maryam, K., Nahid, G., Babak, M., Mohsen, R. 2013. Removal of Methylene Blue from wastewater by adsorption onto ZnCl2 activated Corn Husk carbon : *Equilibrium Studies. Journal of Chemistry,* 2013 :1-6. DOI: http://dx.doi.org/10.1155/2013/383985.

Mekhalef, B.F., Kacha, S.L.A., Belaid, K.D. 2018. Étude comparative de l'adsorption du colorant Victoria Bleu Basique à partir des solutions aqueuses sur du carton usagé et de la sciure de bois. Revue des sciences de l'eau / *Journal of Water Science,* 31(2): 109–126. DOI: https://doi.org/10.7202/1051695ar.

Mekky, A.E.M., El-Masry, M.M., Khalifa, R.E., Omer, A.M., Tamer, T.M., Khan, Z.A., Gouda, M., Mohy, Eldin M.S. 2020. Removal of methylene blue dye from synthetic aqueous solutions using dimethylglyoxime modified amberlite IRA-420: kinetic, equilibrium and thermodynamic studies. Desalination and Water Treatment, 181 : 399-411. DOI : 10.5004/dwt.2020.25097.

Merbouh, Ch., Belhsaien, K., Zouahri, A., Iounes, N.2020, Evaluation de la qualité physico-chimique des eaux souterraines au voisinage de la décharge contrôlée Mohammedia-Benslimane: Étude préliminaire. *European Scientific Journal,* 16(6). DOI: http://dx.doi.org/10.19044/esj.2020.v16n6p455.

Mobalaji, M.J., Olatunde, S.D., Joshua, N.E. 2021. Sequestration of hazardous dyes from aqueous solution using raw and modified agricultural waste. *Adsorption Science and Technology,* 2021 :1-21. DOI: https://doi.org/10.1155/2021/6297451.

Musah, B.M., Peng, L., Xu, Y. 2020. Adsorption of methylene blue using chemically enhanced Platanus orientalis leaf powder : kinetics and mechanisms. Nat. Env. &Poll. Tech., 19 (1) : 29-40. www.neptjournal.com.

Narayana, S.K.V., Ravi, V.K. 2019. Adsorption isotherm studies on methylene blue dye removal using naturally available biosorbent. *Rasayan J. Chem.,* 12(4): 2176-2182.DOI:http://dx.doi.org/10.31788/RJC.2019.1245478.

Nigist, A.H., Ali, S.R., Zemene, W.N. 2022. Chemical modification of neem (Azadirachta indica) biomass as bioadsorbent for removal of Pb2+ ion from aqueous wastewater. Adsorption Science & Technology, 2022: 18. DOI :https://doi.org/10.1155/2022/7813513.

Nyakairu, G.W.A., Kapanga, P.M., Ntale, M. , Lusamba , S.N., Tshimanga, R.M., Ammari, A., Shehu, Z. 2024. Synthesis, characterization and application of Zeolite/Bi2O3 nanocomposite in removal of Rhodamine B dye from wastewater. Cleaner Water, 1(2024) :100004. DOI: https : //dx.doi.org/10.1016/j.clwat.2024.100004.

Pathania, D., Sharma, S., Singh, P. 2017. Removal of methylene blue by adsorption onto activated carbon developed from Ficus carica bast. Arabian journal of chemistry, 10: S1445-S1451. DOI: https: //dx.doi.org/10.1016/j.arabjc.2013.04.021.

Rahimian, R., Zarinabadi, S. 2020. A review of studies on the removal of methylene blue dye from industrial wastewater using activated carbon adsorbents made from Almond

Bark. *Prog. Biochem. Res.,* 3(3): 251-268. DOI : 10.33945/PCBR.2020.3.8.

Raiyyaan, G.D., Khalith, M. S.B., Sheriff, A.M., Arunachalam, K.D.A. 2021. Bio-adsorption of methylene blue dye using chitosan-extracted from Fenneropenaeus indicus shrimp shell waste, *J. Aquac. Mar. Biol.,* 10 (4) : 146-150. https://medcraveonline.com.

Razia, S., Syed, N.T., Usman, T.S., Yunus, K.T.M., Shaik, D.A.K., Imran, M., Kiran, S., Kalam, M.A., Ananda, M.H.C., Akheel, A.S. 2022, Adsorption of Crystal Violet dye from aqueous solution using industrial pepper seed spent: Equilibrium, Thermodynamic, and Kinetic Studies. *Adsorption Science & Technology.,* 2022:ID9009214. DOI:https://doi.org/10.1155/2022/9009214.

Vanessa, P.V., Andrin, A., Le Bechec, M., Lacombe, S., Frayret, J., Pigot, T. 2017. Couplage photocatalytique-oxydation par le ferrate-VI pour le traitement du colorant Rhodamine 6G. Revue des Sciences de l'eau, 30(1):35-39. DOI: https : //dx.doi.org/10.7202/104006Lar.

Tshene, B.W., Kifuani, K.M., Kifuani, A.K.M., Ngoy, P.B., and Ekoko, G. B. 2024. Adsorption of a basic dye methylene blue in aqueous solution on a bioadsorbent from agricultural waste of Manihot esculanta Crantz. *Int. J. Biol. Chem. Sci.,* 18(3): 1180-1198. DOI: https://dx.doi.org/ 10.4314/ijbcs. v 18i3. 35

****